Characterization of a "Blanch-Blush" Mechano-Response in Palmar Skin

Thomas C. Wright[1], Elizabeth Green[1], James B. Phillips[1], Oksana Kostyuk[1] and Robert A. Brown[1]

Palmar finger skin reacts to extension under mechanical load – blanching over proximal (intercrease skin, ICS) and middle phalanges, while blushing in crease skin (CS), which we have called the Blanch-Blush Reaction (BBR). The idea that the BBR is a result of surface capillary blood flow changes that relate to predictable deformation of aligned collagen matrices under applied uniaxial loads was tested. Nondestructive techniques, digital image analysis (DIA), laser Doppler scanning, and elastic scatter spectroscopy (ESS) were used to measure color and blood flow changes in healthy fingers when at rest and extended. Skin strain increased directly with applied load and DIA identified blanching (loss of redness) in the ICS, reflected by a decrease in hemoglobin (by ESS). Laser Doppler flowmetry identified an increase in blood flow in the CS zone on extension, with a minor increase in blood flow in the ICS zone, apparently due to diversion of flow to deeper vessels, when monitored by this technique. These changes correlated with the BBR, owing to altered capillary flow in the ICS and CS. The histology of orientation of collagen fibers and vessels in the two zones was consistent with this mechanism. This study demonstrates the interdependence between matrix orientation, applied load, and flow. It represents an elegant demonstration of collagenous tissue function through an everyday tissue reaction, which has not been described previously.

Journal of Investigative Dermatology (2006) **126,** 220–226. doi:10.1038/sj.jid.5700030

INTRODUCTION

The starting point for this investigation is the novel observation that the Caucasian palm of the hand demonstrates a stretch-sensitive, site-specific color change. When the hand is in the relaxed position, the skin of the palm is a uniform pink color. When the hand is hyperextended, with the fingers stretched out, the palmar skin between joints blanches, and the flexure lines blush red. We have termed this observation the Blanch-Blush Reaction (BBR).

We hypothesize that the visible BBR changes occur as a result of altered superficial blood flow as vessels are constricted or dilated by compaction and separation of the surrounding collagen fibers. The site specificity is likely to be due to the special (predominantly uniaxial) articulation of the digits and the resulting distortion of the palmar dermis collagen matrix in response to mechanical loading.

The structure of the general human dermal microcirculation has been well described using electron microscopy (Yen and Braverman, 1976; Braverman and Yen, 1977; Braverman and Keh-Yen, 1981; Umeda and Ikeda, 1988), light microscopy (Fagrell *et al.*, 1977; Braverman *et al.*, 1990; Braverman, 1997), and laser Doppler flowmetry (Winsor *et al.*, 1987; Braverman *et al.*, 1990; Geirsson *et al.*, 1994; Silverman *et al.*, 1994; Wardell *et al.*, 1994; Braverman, 1997). There are two important plexuses in the dermis: the arterioles and the venules of the cutaneous microcirculation. The upper horizontal network, in the papillary dermis, forms capillary loops to the dermal papillae. The lower horizontal plexus is found between the subcutaneous fat and the deeper reticular dermis. Perforating vessels from underlying muscle and subcutaneous fat form the lower plexus and the arterioles and venules connect directly to the upper plexus, feeding the sweat glands and hair follicles. Most of the dermal microvasculature is contained in the upper plexus and the capillary loops, 1–2 mm below the epidermal surface (Thomine, 1981; Braverman, 1997).

It was important, for the study of the BBR, to use real-time noninvasive analyses as this is a dynamic process linked to a normal function, which cannot be deduced from routine histological techniques. Laser Doppler flowmetry has been used to monitor the underlying microvasculature of skin of the back, chest, and abdomen (Braverman *et al.*, 1990). This technique is particularly useful on flat surfaces and correlates well with results from venous occlusion plethysmography, for measurement of the volume rate of blood flow (Winsor *et al.*, 1987).

Elastic scattering spectroscopy (ESS, also known as diffuse reflectance spectroscopy) is a more recent technique with applications in various diagnostic and tissue engineering areas (Feather *et al.*, 1989; Richards-Kortum and Sevick-Muraca,

[1]*Tissue Repair and Engineering Centre, Institute of Orthopaedics and Musculoskeletal Science, University College London, London, UK*

Correspondence: Professor Robert A. Brown, Tissue Repair and Engineering Centre, Institute of Orthopaedics and Musculoskeletal Science, University College London, RNOH, Brockley Hill, Stanmore Campus, London HA7 4LP, UK. E-mail: rehkrab@ucl.ac.uk

Abbreviations: BBR, Blanch-Blush Reaction; CS, crease skin; DIA, digital image analysis; DIP, distal interphalangeal; ESS, elastic scatter spectroscopy; ICS, intercrease skin; IHb, index of hemoglobin

Received 18 April 2005; revised 22 June 2005; accepted 2 July 2005

1996; Meglinsky and Matcher, 2001; Marenzana *et al*., 2002; Kostyuk and Brown, 2004; Kostyuk *et al*., 2004). Light of visible and near-infrared wavelengths is delivered to the surface of the tissue under investigation, where it is either scattered within the tissue or absorbed (Richards-Kortum and Sevick-Muraca, 1996; Nickell *et al*., 2000). A detecting optical fiber then collects that which is backscattered for analysis in a spectrometer. These collected spectra contain quantitative information about the tissue structure and composition. In biological tissues such as the skin, much of the light absorption is due to specific chromophores, predominantly water, oxyhemoglobin, deoxyhemoglobin, and melanin. Previous studies have described the use of spectroscopic techniques to quantify the relative composition of tissues with respect to these chromophores (Feather *et al*., 1989; Ferguson-Pell and Hagisawa, 1995; Richards-Kortum and Sevick-Muraca, 1996; Haggblad *et al*., 2001; Zonios *et al*., 2001; Sowa *et al*., 2002).

Owing to the predominantly uniaxial loading in the digits, conventional understanding (based on Langer's line concepts (Pierard and Lapiere, 1987)) is that dermal collagen fibril orientation tends to be parallel with the finger axis. In contrast, dermal collagen of the creases appears to be aligned perpendicular to the finger axis. The interpretation of the BBR here was that it is a reflection of the interplay of dermis fiber anisotropy and mechanical loading on vascular flow (hence with a hemoglobin color read-out). The aim of this study was to investigate how the physiology and the microanatomy of skin over the flexure lines might affect the blood flow of the hand with reference to local tensions, and hence the deformation of the collagen network. Collagen orientation and blood flow each influence the results of wound healing, so the understanding of the nature of this phenomenon may prove valuable in understanding normal dermal function and repair.

RESULTS

When the hand is in the relaxed position, the skin of the palm is a uniform pink color. When the hand is hyperextended, with the fingers stretched out, the palmar skin between joints blanches, and the flexure lines blush red. We have termed this observation the BBR. The BBR is a benign event, seen in the hands of all Caucasians so far studied, but obscured by overlaying skin pigmentation. The phenomenon described here is clearly visible to the naked eye as an optical change in color of skin tone in the two regions on extension of the finger. The measurements made here were designed both to quantify this effect and to test how it may operate in terms of superficial blood flow.

Digital image analysis

Digital image analysis (DIA) provides a direct assessment of the visual surface color changes. Figure 1 shows the direct and close relationship between loading weight at the distal interphalangeal (DIP) joint and the strain measured at the skin surface. Linear regression analysis of the mean data showed a statistically significant relationship between applied weight and strain ($r^2 = 0.990$, F-test, $P < 0.0001$), with a strain

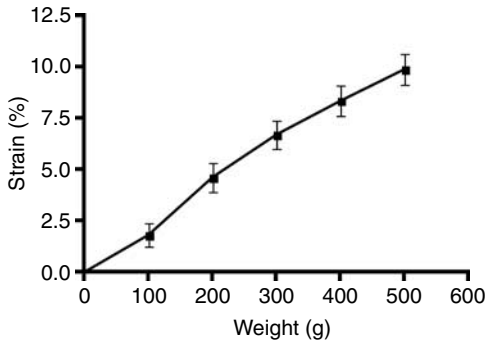

Figure 1. Graph showing the relationship between loading weight and skin surface strain (means ± SEM, $n = 24$).

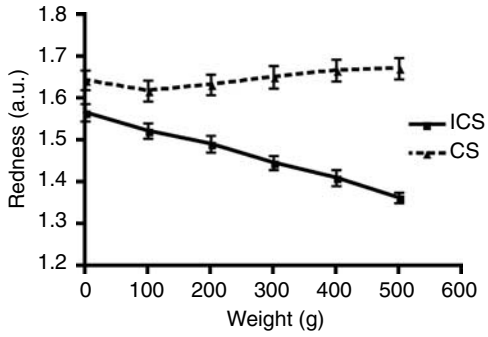

Figure 2. Graph showing the relationship between loading weight and redness in both the CS and ICS zones (means ± SEM, $n = 24$). Redness measured by DIA from the ratio of red:green pixel intensity.

increase of 2.04% (95% confidence interval 1.76–2.32) per 100 g of weight. A maximum strain of 10% was produced using 500 g loading.

Figure 2 shows how application of this strain affected the surface red color in both the intercrease skin (ICS) and crease skin (CS) zones. Redness in the ICS (based on the red/green pixel intensity ratio) zone decreased significantly and linearly under increasing load with an overall reduction of 13% between 0 and 500 g (ICS linear regression analysis gave $r^2 = 0.998$, F-test, $P < 0.0001$). Redness decreased by 0.0401 arbitrary units (a.u.) (95% confidence interval 0.0428–0.0373) per 100 g of weight. In contrast, the small increase in redness in the CS zone was not statistically significant. However, it was visually apparent that redness in the CS was already present in the flat hand position (ie extended in position but with 0 g applied load).

Laser Doppler scanning

The mean blood flow was compared in the relaxed and extended position for both the CS and ICS zones (Figure 3). Overall flow increased significantly on extending the finger in both ICS and CS zones by 17 and 62%, respectively (paired *t*-test, ICS $P = 0.021$, CS $P < 0.0001$).

Hence, the increase in CS blood flow was almost 4-fold greater than in the ICS. Importantly, total mean flow in the ICS of the relaxed hand was almost twice that in the CS, even though there is little visible color difference. Local differences in interstitial fluid can contribute to the laser Doppler signal,

sometimes making a direct comparison between two sites inappropriate, so this observation should be treated with caution. The small (17%) increase in flow in the ICS under extension conflicts with the blanch effect seen visually. This is likely to be a result of the greater vessel density in the deeper soft tissues (particularly subcutaneous fat) of the ICS. The sampling depth of this technique is several millimeters, taking in the full soft tissue layers found only under the ICS, yet changes in this deeper blood flow would have little or no perceivable effect on the visual appearance at the skin surface. Hence, the laser Doppler scanning technique represents a useful measure of superficial flow in the CS (ie the blush), but a poor reflection of blanching in the ICS, where there are deeper tissues with a responsive blood supply.

Elastic scatter spectroscopy

Changes in the index of hemoglobin (IHb) with loading determined for the ICS and CS zones (Figure 4) mirrored the changes seen using DIA. Loading dramatically decreased the IHb of the ICS (linear regression: $r^2 = 0.982$, F-test, $P = 0.0001$) with a total fall of 63% over the range. IHb decreased by 0.0243 arbitrary units (95% confidence interval 0.0288–0.0197) per 100 g of weight. As with redness (measured by DIA), the small increase in IHb in the CS zone was not statistically significant.

Histological analysis

In the ICS region, there was a 3.3-fold greater proportion of axial over transaxial vessels (Mann–Whitney test, $P < 0.0001$). In the CS, this ratio was reversed with 3.3-fold more vessels being transaxial than axial (Mann–Whitney test, $P < 0.0001$). In other words, vessels in the ICS were predominantly parallel to the finger axis, whereas those in the CS were predominantly parallel to the crease lines and therefore perpendicular to the finger axis (Figure 5).

In addition, it was notable that in the CS region there was an obvious increase in blood vessel size directly under the crease compared to the ICS region where blood vessel size was more uniform.

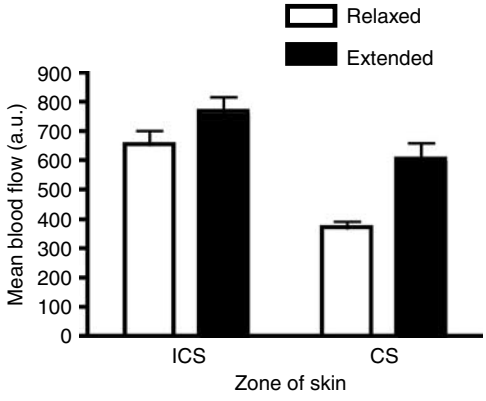

Figure 3. Graph showing the increase in blood flow in the relaxed and extended fingers of the CS and the ICS regions measured by laser Doppler scanning (means ± SEM, $n = 36$).

In nine of 11 ICS sections, the collagen fiber orientation was scored as parallel to the long axis of the finger, whereas in eight of 11 CS sections, fiber orientation was perpendicular or transaxial to the finger (Figure 6). This was a statistically significant difference using Fisher's exact test ($P < 0.0001$). A small proportion of mixed orientation specimens (no predominating alignment) were found but, importantly, the opposing orientation never dominated.

The dermal thickness in the ICS and CS regions was compared to discount this as a possible contributing factor to the visible color changes. The thickness ranged from 0.2 to 1.2 mm in the sections that crossed the CS and from 0.2 to 1.1 mm in the ICS sections, with no statistically significant difference between the two zones.

All of the ICS sections ($n = 12$) were found to have fat beneath the entire section, while only two out of 10 of the CS sections had any underlying fat (Figure 7). This difference was statistically significant (Fisher's exact test, $P = 0.0001$). Control sections (from the skin of the upper arm) ($n = 2$) demonstrated a clear discrete fat layer beneath the reticular dermis, spanning the whole section, comparable with the ICS region. In two of the CS sections (sections too shallow), it was

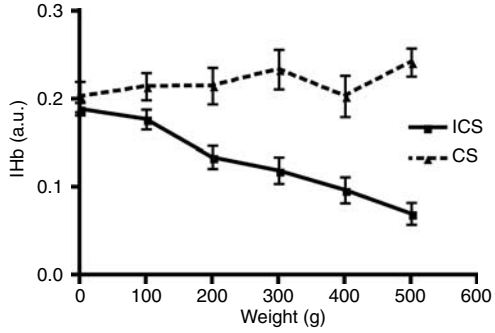

Figure 4. Graph showing the relationship between loading weight and IHb by ESS in both the CS and ICS zones (means ± SEM, $n = 24$).

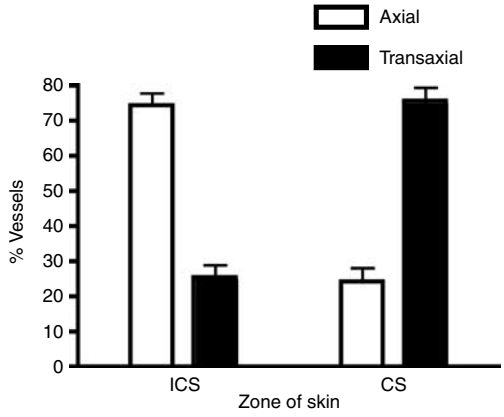

Figure 5. Graph showing the alignment of blood vessels in the ICS and CS zones. The percentage of axial and transaxial vessels in each zone was determined histologically from sections through the skin. Data are means (± SEM) of the percentage values obtained in 12 sections from each zone. (Range of total number of vessels in each section 11–74.) Axis is taken as that of the finger and so of the applied load.

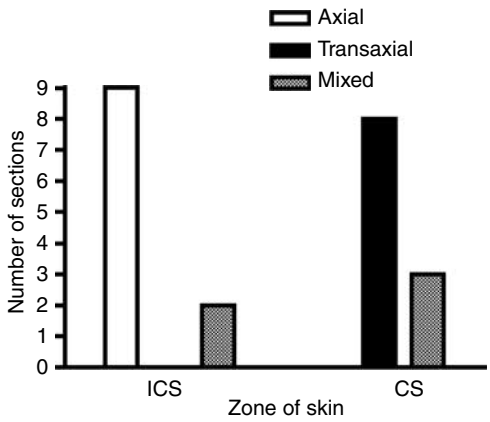

Figure 6. Graph showing the direction of collagen fibers in the ICS and CS zones as determined histologically.

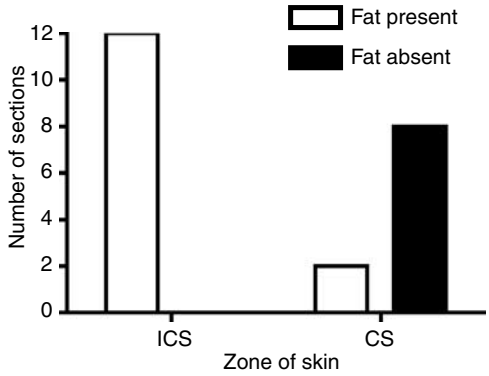

Figure 7. Graph showing the distribution of fat beneath the ICS and CS zones as determined histologically.

not possible to determine the presence of fat below the crease.

DISCUSSION

The aim of this project was to characterize and identify possible mechanisms of action of the BBR in the hand. The study was divided into four areas: DIA, laser Doppler scanning, Elastic scatter spectroscopy (ESS), and histology to relate the underlying anatomy of the surface crease with the changes in blood flow. The palmar aspect of the finger represents one of the simplest joints in the body in that it has a restricted, uniaxial articulation with little rotational movement. The flexure lines of skin are formed when the movement of underlying joints causes skin folding, causing the dermis to attach itself to deeper structures under the skin (Thomine, 1981). The simplicity of articulation in the digits makes it a potential model for helping to understand more complex sites.

The nature of the BBR strongly suggests that it is a visual read-out of the average effect of mechanical tension on the small visible (ie in the upper dermis) blood vessels within the collagen matrix of different fiber orientation. Clearly, a collagenous (fibrous) material such as dermis is anisotropic and so tends to transmit directional loads quite differently in different planes, depending on local fiber orientation. Predictably, this will have distinct effects on embedded microvessels (dilation or constriction) depending on local force and fiber alignment. Significantly, flexor surfaces of the digits undergo tension/compression loading during normal movement, which is almost uniaxial, and this would be predicted to influence local collagen fiber orientation.

From the laser Doppler experiments, it was found that blood flow increased significantly in hyperextension in both the ICS regions and the CS areas. The ICS response initially seemed to contradict the capillary occlusion hypothesis. However, the laser Doppler technique monitored blood flow in tissue up to 3 mm deep (Wardell *et al.*, 1993), well into the subcutaneous fat pad. In the ICS region, this fat layer was rich in blood vessels adjacent to the basal dermis. Clearly then, these vessels contributed strongly to the overall laser Doppler signal, yet the dermis is not translucent at this depth and such vessels will make little contribution to skin color (and so to the BBR). Since there is no subcutaneous fat pad beneath CS zones, this anomaly did not occur and so change in blood flow corresponded with the BBR on hyperextension as expected.

The BBR was clearly visible to the naked eye and so it was expected that DIA would quantify this color change relative to the skin surface strain on loading the finger in extension. Although DIA was able to identify a significant blanching in the ICS region, it did not show any significant blushing in the CS region on loading the finger. A possible explanation for this discrepancy is that in these experiments we were forced to define ''zero loading'' as the finger positioned straight (ie in extension) with no additional applied load as this was effectively the only feasible ''null'' position. It is likely that some blushing occurred on straightening the finger from a truly relaxed position (half-flexed).

ESS analysis showed that IHb was related to loading weight in a very similar way to redness in the DIA experiments. This provides experimental support for the explanation that the BBR color change is due to relative changes in hemoglobin levels in the ICS and CS zones. The source–detector separation of the probe of 600 μm was the narrowest available, and sampled the more superficial tissue of the skin (Meglinsky and Matcher, 2001) (in the order of less than 1 mm). Whereas DIA assessed a two-dimensional image of the skin surface, ESS determined the relative amount of hemoglobin in a superficial, approximately hemispherical volume of skin. The fact that the graphs for redness and IHb so closely mirror each other suggests that the volume of tissue sampled is the superficial papillary dermis, which can be visualized from the surface of the skin. This is in agreement with other studies that have shown that source–detector separations of 400–800 μm principally sample tissue in the upper dermis (Meglinsky and Matcher, 2001). These findings indicate that blood is expelled from the dermal capillaries in the ICS during loading in the BBR, while blood flow in the CS zone continues to flow freely.

The histology findings supported the idea that in the superficial layer of the dermis, blood vessels tend to run

parallel with the collagen fibers, since fiber orientation may give strong tissue guidance. The finding that there was a significant difference in blood vessel orientation in the CS and ICS regions is crucial here. Specifically, crease blood vessels tended to run across the digit, while ICS blood vessels ran along the digit. This distribution was predicted by, and also strongly supports, the hypothesis that the BBR is a result of compression and dilation of vessels by aligned collagen fibrils as they are mechanically loaded either parallel or perpendicular to their alignment, respectively. Hyperextension by this mechanism would occlude flow in the ICS region, but dilate blood vessels in the CS region.

The fat distribution beneath the dermis was studied to test the possibility that blanching could be a result of the dermal vascular bed being constricted by compression against hard tissue beneath the dermis. However, fat was considered to be a particularly soft underlying tissue and was shown to have completely the reverse distribution needed for this explanation (ie large soft deposits beneath the ICS but no fat and hence harder tissues directly beneath the creases), this makes the joint and the CS region the hardest part of the finger beneath the skin. The contribution of underlying tissues, then, seems to be unimportant.

In conclusion, the findings of this study support the proposed mechanism for tension-mediated BBR. The close correlation of a visible color change, vascular flow, and axial tension with collagen fiber alignment makes the BBR a potentially important phenomenon. Firstly, it is informative in terms of normal tissue architecture and perfusion at the cell and fiber level (important in current tissue repair and tissue engineering research). Secondly, the BBR offers unique potential as a simple noninvasive means of monitoring dysfunctional and age-related dermal and capillary function, with considerable diagnostic potential.

MATERIALS AND METHODS

Digital image analysis

The medical ethical committee of University College London approved all described studies and the study was conducted according to the Declaration of Helsinki principles. Each experimental subject was given verbal information about the project aims and experimental methodology before giving verbal consent.

Six Caucasian volunteers were investigated (three women and three men, age range 21–34 years). Photographic images were obtained of each subject's index and ring finger on the left and right hand, with a scale bar for calibration. Two marker points were then marked on each finger 10 mm proximal and distal to the most proximal of the proximal interphalangeal skin creases in the mid-axial line.

Three images were captured for each finger at rest ($n = 24$), and under increasing increments of hyperextension using a microscopic digital video camera (Scopeman® 504, Moritex, Cambridge, UK) at $\times 10$ magnification (focal distance 70 mm), with image capture to a laptop PC and image analysis using Adobe Photoshop 7.0 software. Hyperextension at the metacarpophalangeal joint was achieved by hanging a series of weights (0–500 g at 100 g increments) from the DIP crease. The forearm was maintained in a constant position throughout the loading and the weights were suspended from the DIP crease using a narrow (1 mm) latex loop to ensure consistent loading.

Strain analysis

For each loading, the change in distance between the marker points was measured between rest (zero loading, zero strain) and under the applied load:

$$\%\,\text{Strain} = \Delta d/d_0 \times 100$$

where d_0 is the distance between marker points at zero loading and Δd is the change in distance from zero loading to loaded.

Color analysis

Change of skin color in each test area image was assessed by sampling eight areas of 5×5 pixels both in the crease and in the ICS regions. The sampling areas were taken at regular equal distances along two 4 mm long transect lines – one over the most proximal proximal interphalangeal crease and one 8 mm proximal to this – both perpendicular to the mid-axial line. Average intensity of red, green, and blue in each area was found. The greatest color difference between the two regions was found to be the ratio of red to green and it was this ratio that was used as a measure of ''redness'' in the two regions.

Laser Doppler scanning experiments

Five Caucasian volunteers were investigated (four women, one men, age range 22–40 years) and the blood flow within the dermis of the hand was measured using a laser Doppler scanner (Moor Instruments Ltd, Axeminster, UK). Four scans were completed on the palmar aspect of both hands of each subject when relaxed and extended.

To ensure consistency, a 200 g weight was suspended from the DIP crease of the index finger and the subject was then asked to hyperextend the other three fingers. The metacarpophalangeal joint of the index finger was immobilized during hyperextension to further standardize the experiment.

The images of the scans were analyzed to give a relative measure of blood flow through the surface of the scanned fingers. The blood flow of the proximal interphalangeal creases was obtained by placing the pixel of the analysis system at three points along the crease as shown in Figure 8. The mean blood flow of the ICS regions was measured by calculating the mean blood flow of the skin within a box drawn onto the image of the ICS region.

Elastic scatter spectroscopy

These experiments were carried out on the same cohort of volunteers sampling from the same fingers and with the same loading regimes as the DIA. The equipment used consisted of an optical probe connected to a light source and spectrometer, and controlled by a laptop PC for data acquisition. The optical probe contained two fibers: one (the source) delivered white light from a xenon-arc lamp and the second (the detector) collected backscattered light. Spectra were analyzed using a spectrometer (Ocean Optics, Dunedin, FL) for detection over the range of 300–900 nm. The probe itself was cylindrical, 6 mm in diameter with a source–detector (centers) separation of 600 μm. Typical data acquisition and display took less than 1 second for each measurement. To take into account the spectral characteristics and overall intensity of the lamp, a spectrum

of the diffuse reflectance standard (Ocean Optics, Florida) recorded prior to each measurement session was used as a reference.

Readings were taken from each finger (same protocol as for DIA experiments) over both the ICS and CS zones, at rest and with weights hung from the DIP joint (0–500 g in 100 g increments). The probe was positioned such that the detector fiber and the source fiber were orientated over the mid-axial line of the finger. To standardize the sampling, readings from the CS were taken with the center of the probe over the most proximal proximal interphalangeal crease and those from the ICS were taken 8 mm proximal to this. The probe was positioned to be ''just touching'' the skin (reported by the subject), and perpendicular to the palmar surface. Three spectra were obtained for each finger and each position to give an average spectrum with which to determine the relative amounts of hemoglobin in the tissues sampled. Spectra were converted into absorption mode using the formula (Dawson *et al.*, 1980; Feather *et al.*, 1989):

$$\text{absorption} = \log_{10}(1/\text{backscatter intensity})$$

Blood content was then quantified by using a previously validated technique (Feather *et al.*, 1989; Hagisawa *et al.*, 1994). The mean IHb was calculated for each load and both zones using the formula:

$$\text{IHb} = [((A_{546} - A_{521})/25) - ((A_{566} - A_{546})/20)] \times 50$$

where A_x is the absorption intensity at wavelength $\times$ nm.

The laboratory temperature was measured to be 22–23°C for all experiments.

Histology

Skin specimens were taken from the ICS regions, or proximal interphalangeal or DIP creases on the volar surface of 10 cadaveric fingers. Specimens were routinely formalin-fixed, dehydrated, wax-embedded, and sectioned (3 μm) for staining with Masson's trichrome to determine (i) collagen fiber orientation, (ii) the fat distribution beneath the dermis, (iii) dermal thickness, and (iv) blood vessel size, direction, and density. All specimens were examined directly under light microscopy (Olympus Diaphot, Nikon, Japan). Measurements were taken using an eyepiece graticule.

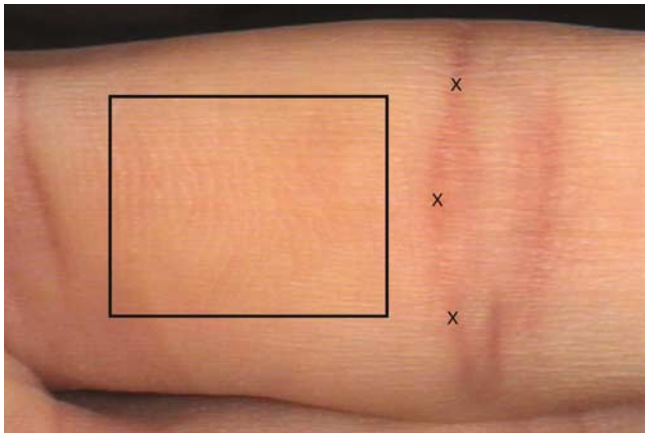

Figure 8. Image of finger in extension. The rectangle indicates laser Doppler blood flow sampling in the ICS zone and $\times$ represents positions of sampling for the CS zone. Blanching of the ICS zone is apparent grossly within the box. The blush reaction of the CS zone is also clearly visible. At rest, the color of both ICS and CS zones is approximately the same, pale pink (not shown).

The sections from the CS region were cut parallel to, and those from the ICS were cut perpendicular to, the axis of the finger. Blood vessels in histological sections of the CS and ICS with orientations parallel or perpendicular to the finger axis were counted. Those blood vessels that were either round or ovoid in shape were classified as axial in the ICS sections and as transaxial in the CS region. Vessels seen in longitudinal section (ie with a length to width ratio of 3 or more) were classified as transaxial in the ICS sections and axial in the CS sections. In order to distinguish between collagen fiber orientations (relative to the long axis of the finger), we termed the fibers transaxial if they ran across the section and axial if they appeared round or oval in section for the ICS sections and the reverse for fibers in the CS regions. Fibers were mixed if neither direction predominated.

CONFLICT OF INTEREST

The author states no conflict of interest.

ACKNOWLEDGMENTS

We are grateful to EPSRC and the Middlesex Hospital Trust Clinical Research Fund for part funding, to Drs Paul Banwell and Erik Walbeehm for their invaluable assistance with Doppler and tissue analysis.

REFERENCES

Braverman IM (1997) The cutaneous microcirculation: ultrastructure and microanatomical organization. *Microcirculation* 4:329–40

Braverman IM, Keh A, Goldminz D (1990) Correlation of laser Doppler wave patterns with underlying microvascular anatomy. *J Invest Dermatol* 95: 283–6

Braverman IM, Keh-Yen A (1981) Ultrastructure of the human dermal microcirculation. III. The vessels in the mid- and lower dermis and subcutaneous fat. *J Invest Dermatol* 77:297–304

Braverman IM, Yen A (1977) Ultrastructure of the human dermal microcirculation. II. The capillary loops of the dermal papillae. *J Invest Dermatol* 68:44–52

Dawson JB, Barker DJ, Ellis DJ, Grassam E, Cotterill JA, Fisher GW *et al.* (1980) A theoretical and experimental study of light absorption and scattering by *in vivo* skin. *Phys Med Biol* 25:695–709

Fagrell B, Fronek A, Intaglietta M (1977) A microscope–television system for studying flow velocity in human skin capillaries. *Am J Physiol* 233: H318–21

Feather JW, Hajizadeh-Saffar M, Leslie G, Dawson JB (1989) A portable scanning reflectance spectrophotometer using visible wavelengths for the rapid measurement of skin pigments. *Phys Med Biol* 34:807–20

Ferguson-Pell M, Hagisawa S (1995) An empirical technique to compensate for melanin when monitoring skin microcirculation using reflectance spectrophotometry. *Med Eng Phys* 17:104–10

Geirsson AJ, Jonsson GS, Asgeirsdottir LP (1994) Functional study of the dermal microcirculation in systemic sclerosis. *Scand J Rheumatol* 23: 73–6

Haggblad E, Larsson M, Arildsson M, Stromberg T, Salerud EG (2001) Reflection spectroscopy of analgesized skin. *Microvasc Res* 62:392–400

Hagisawa S, Ferguson-Pell M, Cardi M, Miller SD (1994) Assessment of skin blood content and oxygenation in spinal cord injured subjects during reactive hyperemia. *J Rehabil Res Dev* 31:1–14

Kostyuk O, Birch HL, Mudera V, Brown RA (2004) Structural changes in loaded equine tendons can be monitored by a novel spectroscopic technique. *J Physiol* 554:791–801

Kostyuk O, Brown RA (2004) Monitoring of the alignment in developing tissue-engineered constructs by elastic scattering spectroscopy. *Proc SPIE* 5486:198–202

Marenzana M, Pickard D, MacRobert AJ, Brown RA (2002) Optical measurement of three-dimensional collagen gel constructs by elastic scattering spectroscopy. *Tissue Eng* 8:409–18

Meglinsky IV, Matcher SJ (2001) Modelling the sampling volume for skin blood oxygenation measurements. *Med Biol Eng Comput* 39:44–50

Nickell S, Hermann M, Essenpreis M, Farrell TJ, Kramer U, Patterson MS (2000) Anisotropy of light propagation in human skin. *Phys Med Biol* 45:2873–86

Pierard GE, Lapiere CM (1987) Microanatomy of the dermis in relation to relaxed skin tension lines and Langer's lines. *Am J Dermatopathol* 9: 219–24

Richards-Kortum R, Sevick-Muraca E (1996) Quantitative optical spectroscopy for tissue diagnosis. *Annu Rev Phys Chem* 47:555–606

Silverman DG, Jotkowitz AB, Freemer M, Gutter V, O'Connor TZ, Braverman IM (1994) Peripheral assessment of phenylephrine-induced vasoconstriction by laser Doppler flowmetry and its potential relevance to homeostatic mechanisms. *Circulation* 90:23–6

Sowa MG, Matas A, Schattka BJ, Mantsch HH (2002) Spectroscopic assessment of cutaneous hemodynamics in the presence of high epidermal melanin concentration. *Clin Chim Acta* 317:203–12

Thomine J-M (1981) The skin of the hand. In: *The Hand* (Tubiana R, ed), 1st ed. Philadelphia: W.B. Saunders Company, 107–15

Umeda N, Ikeda A (1988) Scanning electron microscopic study of the capillary loops in the dermal papillae. Skin of the hand of the Japanese monkey (*Macaca fuscata*). *Acta Anat (Basel)* 132:270–5

Wardell K, Braverman IM, Silverman DG, Nilsson GE (1994) Spatial heterogeneity in normal skin perfusion recorded with laser Doppler imaging and flowmetry. *Microvasc Res* 48:26–38

Wardell K, Jakobsson A, Nilsson GE (1993) Laser Doppler perfusion imaging by dynamic light scattering. *IEEE Trans Biomed Eng* 40:309–16

Winsor T, Haumschild DJ, Winsor DW, Wang Y, Luong TN (1987) Clinical application of laser Doppler flowmetry for measurement of cutaneous circulation in health and disease. *Angiology* 38:727–36

Yen A, Braverman IM (1976) Ultrastructure of the human dermal microcirculation: the horizontal plexus of the papillary dermis. *J Invest Dermatol* 66:131–42

Zonios G, Bykowski J, Kollias N (2001) Skin melanin, hemoglobin, and light scattering properties can be quantitatively assessed *in vivo* using diffuse reflectance spectroscopy. *J Invest Dermatol* 117:1452–7